Mechanisms of failure in porcelain-veneered sintered zirconia restorations

Tan Sui[1,*], Kalin Dragnevski[1], Tee K. Neo[2,3], Alexander M. Korsunsky[1]

[1] Department of Engineering Science, University of Oxford, Parks Road, Oxford OX1 3PJ, United Kingdom
[2] Specialist Dental Group, Mount Elizabeth Medical Centre, 3 Mount Elizabeth, #08-08/08-10, Singapore 228510, Singapore
[3] Faculty of Dentistry, National University of Singapore, 11 Lower Kent Ridge Road, Singapore 119083, Singapore
* Corresponding author: tan.sui@eng.ox.ac.uk

Abstract The continuous increase in the demand for highly aesthetic and natural-appearing dental restorations and the development of strong ceramic materials has led to the adoption of sintered ceramics as new load-bearing components used in dental prosthetics. Zirconia is one of the most attractive restorative materials due to its advantageous mechanical properties and biocompatibility. Veneering porcelains are used to coat the surface of zirconia to enhance the aesthetic appearance of prostheses. Nevertheless, porcelain-veneered zirconia restorations are prone to failure primarily by the fracture of the veneering layers. In this paper, the nature of the interfacial bonding and failure modes on samples of broken porcelain-veneered sintered zirconia restorations were studied using Environmental Scanning Electron Microscopy (ESEM) with Energy-Dispersive X-ray (EDX) analysis. Typical fractographic features were observed in broken porcelain-zirconia prosthesis. The chipping mode fractures in the veneering porcelain indicated the dominance of the cohesive fracture mode, in agreement with clinical experience reported in the literature. The crack initiation and propagation within the veneered porcelain layer was also observed and analyzed by a further examination of the fractographic features on both the prosthetic samples and the fractured surface of porcelain zirconia bars. The result indicates that the crack initiated at the location of maximum stress (point of occlusal contact). In addition, it is surmised that the fragility of the prosthesis may result from the high Vickers hardness and the associated low toughness of porcelain.

Keywords zirconia-based dental prosthesis, interface bonding, failure mode, mechanical properties

1. Introduction

Recent decades witnessed a continuous and considerable increase in the demand for highly aesthetic and natural-appearing dental restorations. At the same time, development of strong engineering ceramic materials took place. The above trends led to the adoption of sintered ceramics as new load-bearing components used in dental prosthetics [1]. Zirconia is one of the most attractive restorative materials due to its advantageous mechanical properties, biocompatibility and aesthetic appearance. Veneering porcelains with mechanical properties inferior to zirconia are used to coat the surface of zirconia to enhance the natural appearance of prostheses [2-4]. Nevertheless, porcelain-veneered zirconia restorations are prone to failure primarily by the fracture of the veneering layers [5]. This has been the dominant clinically observed failure mode, also called chipping mode failure [5,6]. One measure of the liability of dental ceramics to failure is fracture toughness, defined as the critical stress intensity factor at which a crack starts to propagate, and used as a measure of the resistance to catastrophic failure [7-9]. Possible procedures used to enhance the fracture toughness of veneering ceramics, without compromising their hardness, are likely to help reduce the incidence of such failures in clinical practice.

In this paper, the fractured surface of porcelain-veneered sintered zirconia prosthesis samples was examined under Environmental Scanning Electron Microscopy (ESEM) with Energy-Dispersive X-ray (EDX) analysis in order to identify the crack initiation sites and the propagation direction based on the observed fractographic features [10]. To validate further, the observed crack initiation features, some specially fabricated samples in the form of zirconia-porcelain bars were broken by three-point bending, and the fracture surfaces examined under ESEM. Vickers indentation was also

carried out in the attempt to explain the fragility of the porcelain.

2. Experimental procedure

Two samples (designated “prosthesis #1 and #2”) of porcelain-veneered sintered zirconia restorations were supplied for analytical examination as examples of clinical failure. Fig.1 illustrates the failure mode primarily confined to the porcelain veneer and commonly referred to as “chipping”. Fig.1(a) shows the image of prosthesis #1 taken with the fractured unit when still mounted in the oral cavity (9, left maxillary central incisor), whilst Fig.1(b) shows a similar chipping failure in the veneering porcelain on the upper 1st molar.

(a) (b)

Figure 1 Porcelain-veneered sintered zirconia restoration.
(a) fractured unit mounted in the oral cavity; (b) chipping failure on the upper 1st molar.

Energy-Dispersive X-ray (EDX) analysis is a technique for surface examination conducted within the Environmental Scanning Electron Microscopy (ESEM) vacuum chamber and allows the determination of specific elemental composition at high spatial resolution. ESEM with EDX analysis was firstly carried out on the prosthesis samples (Fig. 1) to investigate the nature of interfacial bonding and fracture features in order to identify the crack initiation sites and propagation directions. To investigate further the fracture mechanism and material properties, nine cylindrical porcelain-veneered zirconia bars were fabricated, three of which (designated “bar #1-#3”) were fractured by three-point bending. The fractured surfaces were studied by ESEM, while the other six bar samples (designated “Vickers #1-#6”) were indented by Vickers hardness testing machine. The corresponding Vickers hardness and toughness values were evaluated with the aid of ESEM imaging.

3. ESEM characterization of prosthesis samples

3.1. Interfacial bonding

EDX is useful in determining elemental distribution of materials, and thus the mutual elemental diffusion can be identified. In the present study, EDX analysis was conducted on the broken surfaces within the region shown in Fig. 2(a). The results indicate that the porcelain region contains a high overall concentration of O and silicon (Si), due to the high silica (SiO_2) content. Notably, there is evidence of not only Si diffusing into the Zr-rich domain (Si map), but also zirconium (Zr) diffusing into the Si-rich porcelain domain (Zr map). This evidence of mutual elemental diffusion of Zr and Si reveals the origins of the good mechanical bonding observed between zirconia ceramic copings and porcelain veneers [11-13]. It is also worth noting that the studies of fracture surfaces of the sample supplied failed to identify prominent cases of adhesive fracture localized along the

interface (that is marked with an arrow). The combination of these observations suggests that the interfacial bonding between zirconia and porcelain can be classified as strong.

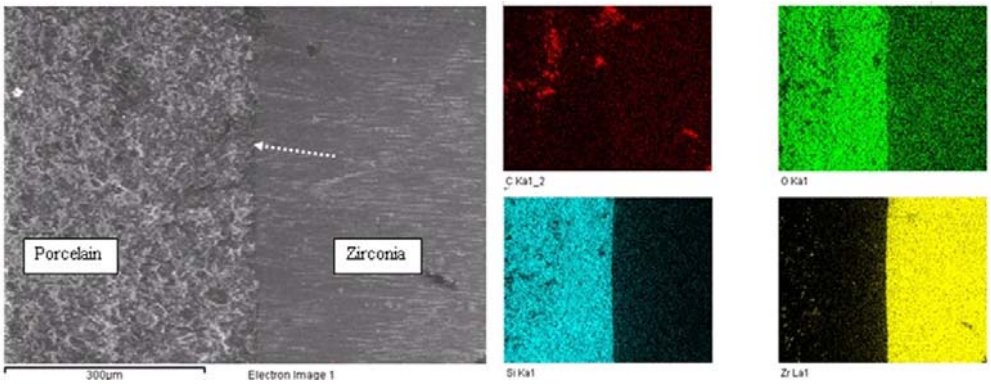

(a) (b)

Figure 2 ESEM image and corresponding elemental X-ray maps of the region of interfacial bonding

3.2 Pre-existing defects

The preparation procedure used for porcelain naturally leads to the formation of gas bubbles that persist as defects within the veneering layer. This may increase the likelihood of crack initiation at these positions under the applied mastication load, and may lead to chipping mode cracking in which the fracture propagates by connecting different defects. Fig. 3 illustrates the presence of the pre-existing pores of a range of sizes within prosthesis #1. The SEM image shown was collected from the occlusal-facing fracture surface remaining after chipping. The characteristic semi-spherical smooth dimples represent the remainder after the passage of a crack through pre-existing pores. The presence of both large pores (>20μm) and smaller pores (~10 μm) is noted. Therefore, it appears that some control over the pore size or the distribution of flaws within porcelain veneer after firing would be helpful in reducing the possibility of crack initiation. Since quality control over individual restorations appears to be prohibitively expensive, this would be probably best exercised through control of the thermal schedules and over the veneer shape and thickness.

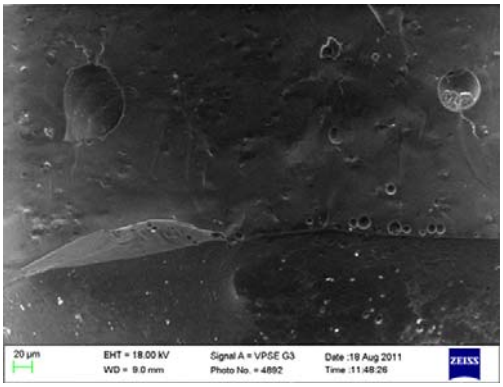

Figure 3 ESEM image of the porcelain fractured surface, showing presence of pre-existing pore defects

3.3 Chipping mode fracture

In most cases, the chippings were contained entirely within the porcelain layer and did not reach the interface with the zirconia core, i.e. the cohesive fracture mode was observed. However, it is conceivable that cracks initiated close to or at the veneering surface may propagate across the unit and through the interface to cause the final failure, in which case the adhesive mode of fracture would be observed. A micrograph of chipping mode failure observed is illustrated in Fig. 4(a). The

cohesive fracture through the porcelain layer is in agreement with literature that crack initiation within the veneered porcelain layer is the dominant failure mode for both metal coping and all-ceramic restorations [14]. Fig. 4(b) illustrates a region of oblique fracture in porcelain that propagated towards and along the interface of the underlying zirconia structure. Further confirmation was sought by EDX analysis. It is apparent that the top left region is Si-rich (porcelain), while the bottom right region is rich in zirconium (core).

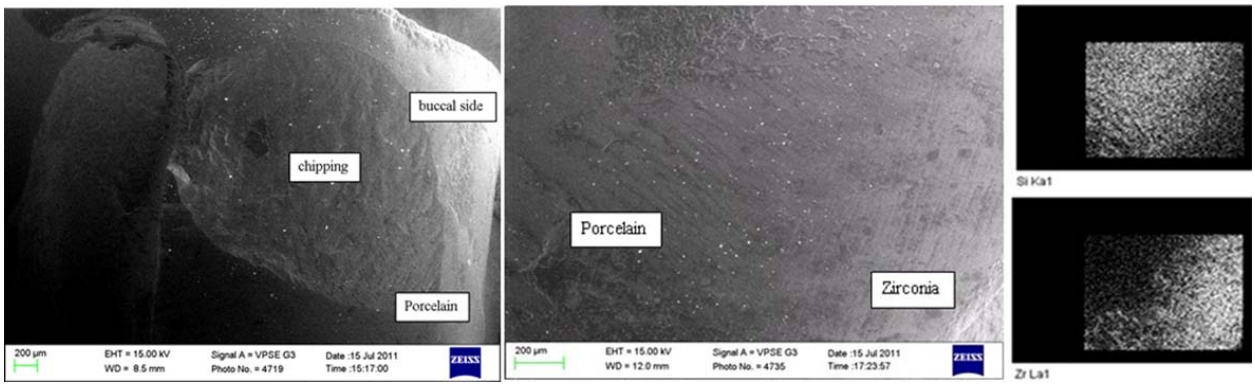

(a) (b)

Figure 4 Typical two fracture modes on the surface of restoration. (a) Overall micrograph of chipping failure; (b) An oblique fracture in porcelain that propagated towards and along the interface with the underlying zirconia core structure

3.4 Crack initiation and propagation

Fractographic analysis was used to determine the crack propagation direction and the crack initiation location by identifying certain common features, namely “wake hackle” and “arrest lines” (identified below in Fig. 5) [15,16]. These were found at the fractured surfaces within the samples investigated in this report, and were used to trace the crack propagation back to the fracture origin. Wake hackle is generally formed when a crack passes a discontinuity, e.g. void. It is associated with the high stress field experienced by the void as the crack propagates close to it. This usually causes crack re-initiation at a point that lies slightly above or below the major crack plane. However, the fastest moving major crack eventually catches up with this new propagating micro-crack, and the latter becomes incorporated in the master crack. Meanwhile, a tell-tale surface hollow or elevated region is left behind, which is referred to as the “wake hackle”, pointing in the direction of crack propagation. Arrest line is another indicator of the crack propagation direction. It is approximately perpendicular to the general direction of propagation. Since the growing crack expands in different directions during growth, the crack origin lies behind the concave side of the crack front. Hence, the fracture origin can be traced back to the approximate center of expanding arrest lines family observed at the fracture surface [17].

Fig. 5 shows the surface of a porcelain-initiated fracture in the chipping on the surface of prosthesis #2, with crack initiated at defects in the veneer located at or close to the occlusal surface. The region indicated by the rectangular white box in Fig. 5(a) is shown at higher magnification in Fig. 5(b), where the wake hackle and arrest line features are identified. Fractographic analysis shows that crack may progress from two origins (Fig. 5(a)) lying on the left of the picture, within the porcelain veneer layer and at or close to the surface. Hence we draw the conclusion that fracture initiated close or at the veneer surface, and propagated across the unit and through the interface to cause final failure. Meanwhile, material aspects (coefficients of thermal expansion, thermal conductivity mismatch, phase transformation [18,19]) of porcelain close to the surface may give rise to residual stresses throughout the restoration that likely to promote chipping.

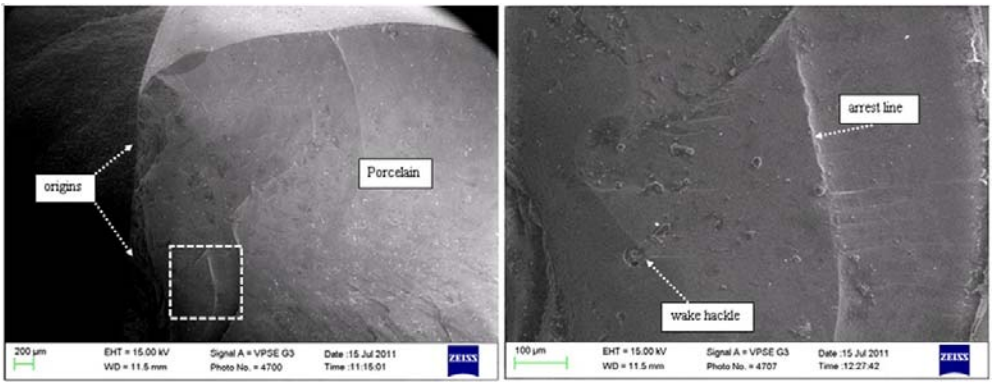

(a) (b)

Figure 5 Fractographic features in porcelain layer of prosthesis #2. (a) Surface of a porcelain-initiated fracture in the chipping on the surface; (b) Higher magnification image of the highlighted (white dashed square) region in (a)

In the case of prosthesis #1, considering the junction between the occlusal fractured surface and the lingual side of the restoration, we conclude that the crack initiation may have occurred at this junction and propagated from the junction to the occlusal surface, roughly from left to right in Fig. 6. The short dashed arrows on the lingual side are considered as the candidate sites for crack initiation, and longer dashed arrows on the occlusal side indicate the putative crack propagation direction. Thus, the crack may initiate on the lingual side with a concentrated force perpendicular to the lingual side, which leads to the crack initiation and propagation on the cross section, i.e. occlusal side, and final breakage. It is worth noting the change of direction of the crack that is seen in Fig. 6. This is likely to indicate a transition from friction-assisted cone crack induced by the grinding contact at the porcelain surface, to faster pressure-induced tensile fracture mode that leads to the subsequently observed fracture [5].

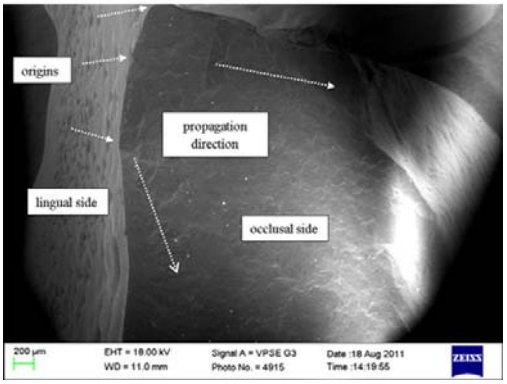

Figure 6 Fractographic features in porcelain layer of prosthesis #1

4. ESEM characterization of broken porcelain-zirconia bars

4.1 Fractured surface after three-point bending

To validate the above observations made on prostheses samples, three-point bending was carried out on three zirconia-porcelain bars and the fractured surface was examined by means of ESEM. A schematic diagram of the three-point bending experiment is shown in Fig. 7(a). As a brittle material, the porcelain fails most readily in tension. The crack is expected to initiate from the location of maximum tensile stress, i.e. the “top” position (marked with yellow circle in Fig. 7(a)). This was

verified by the detailed analysis of fractographic features shown in Figs. 7(b) and 7(c) (images of one representative sample) that indicate the crack propagation from “top” to “bottom” (marked with white dashed arrow Fig.7(b)), although the features were only visible on the “left” and “right” sides, or both sides of the cross section (marked with red circle in Fig. 7(a)) due to the breakaway of the porcelain on the “top” or “bottom” sides.

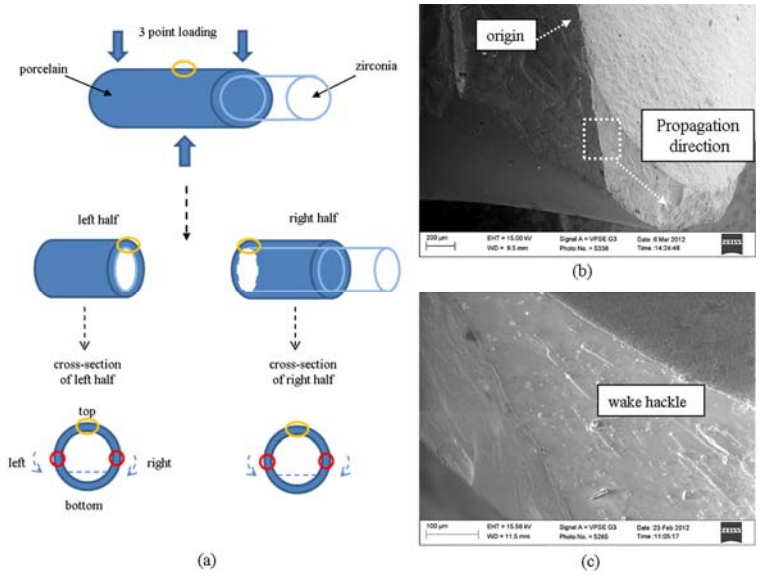

Figure 7 Schematic representation of the three-point bending test and failure of the specimens
(a) three-point bending; (b) & (c) typical ESEM images of the fractured surfaces

4.2 Vickers hardness and toughness evaluation

Further evaluation of the mechanical properties of the veneering porcelain (hardness and fracture toughness) was carried out using Vickers indentation on six zirconia porcelain bar samples (designated “Vickers #1-#6”). The formulas used for the evaluation of Vickers hardness and toughness are [8,20,21].

$$H = \frac{F}{A} = \frac{1.854F}{d^2} \tag{1}$$

$$K_{IC} = 0.016\left(\frac{E}{H}\right)^{0.5}\left(\frac{F}{c^{1.5}}\right) \tag{2}$$

where F is the applied force on the diamond indenter (unit of N), A is the surface area of the resulting indentation (unit mm^2), d the average length of the diagonal left by the indenter (the average of two diagonals d_1 and d_2) with the unit of mm, c the crack size measured from the center of the indentation (unit of mm), H is Vickers hardness (unit of GPa) and E is Young’s modulus (unit of GPa), and K_{IC} is the fracture toughness (unit of MPa/m$^{1/2}$). For illustration, the indentation impression in sample Vickers #1 is shown in Fig. 8. The results of all six indented samples with loads of 10N and 50N are listed in Table 1.

Table 1 Hardness and toughness of the indented samples

Sample	Load (N)	d_1 (μm)	d_2 (μm)	d (μm)	Vickers hardness (GPa)	c (μm)	E (GPa)	Toughness (MPa/m$^{1/2}$)
#1	10	45.96	47.35	46.66	8.516	71.88	65	0.725
#2	10	41.95	44.35	43.15	9.957	56.60	65	0.960
#3	10	39.92	44.66	42.29	10.367	49.62	65	1.146
#4	50	98.68	70.70	84.69	12.925	178.5	65	0.752
#5	50	98.31	104.5	101.405	9.015	182	65	0.875
#6	50	122.1	125.0	123.55	6.073	194.3	65	0.966

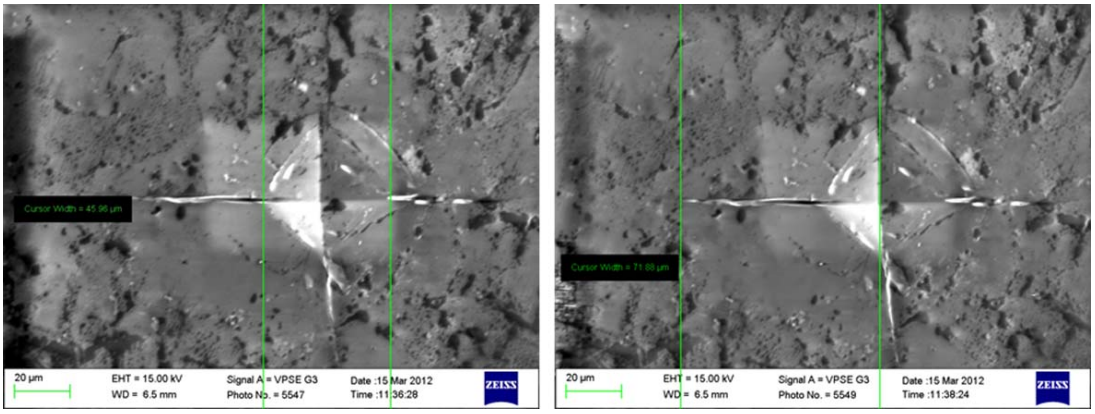

(a) (b)

Figure 8 Vickers hardness and toughness determination for specimen Vickers #1 (10N load) (a) measurement of the diagonal length; (b) measurement of the crack length

In the results found in the literature, the average toughness of porcelain has been reported to lie in the range 1.5-2.1MPa/m$^{1/2}$, and the hardness in the range 4-8GPa [7,9,20,21], the results demonstrate that the porcelain used in this experiment has a relatively high hardness, and accordingly a reduced level of toughness. This may be due to the inherent chemical formulation of the porcelain or its processing history. Notably, merely the presence of a population of voids is likely to result in reduced toughness, but may not lead to increased hardness observed in our experiments.

5. Conclusion

Conclusions are made based on the ESEM and EDX analyses conducted for this paper. The strength of the zirconia-porcelain interface is derived from the mutual diffusion of zirconium and silicon at the interface. Chipping mode fractures observed in the veneering porcelain indicate the dominance of the cohesive fracture. Adhesive fracture may only be observed in the case of crack travelling at a very shallow angle to the interface. Failure of all-ceramic zirconia-based restorations by porcelain veneer chipping is a complex process that depends on a large number of factors. Pre-existing defects in the porcelain veneer may promote chipping mode cracking and final failure. The results from fractured surface examination of the porcelain zirconia bars further confirm that in the real prosthesis the crack is likely to initiate at the position in lingual side with maximum stress. Moreover, great Vickers hardness and low toughness suggest the weakness of porcelain. Exercising control over these fabrications appears to be a critical requirement for clinical practice.

Acknowledgements

The authors would like to thank Igor N Dyson for his great help in performing the three-point bending and Vickers indentation.

References

[1] F. Zarone, S. Russo, R. Sorrentino, From porcelain-fused-to-metal to zirconia: Clinical and experimental considerations, Dent Mater, 27 (2011) 83-96.

[2] H.M. Al-Dohan, P. Yaman, J.B. Dennison, M.E. Razzoog, B.R. Lang, Shear strength of core–veneer interface in bi-layered ceramics, J Prosthetic Dent, 91 (2004) 349-355.

[3] M. Guazzato, K. Proos, L. Quach, M.V. Swain, Strength, reliability and mode of fracture of bilayered porcelain/zirconia (Y-TZP) dental ceramics, Biomaterials, 25 (2004) 5045-5052.

[4] G. Isgro, P. Pallav, J.M. van der Zel, A.J. Feilzer, The influence of the veneering porcelain and different surface treatments on the biaxial flexural strength of a heat-pressed ceramic, J Prosthetic Dent, 90 (2003) 465-473.

[5] E.D. Rekow, N.R.F.A. Silva, P.G. Coelho, Y. Zhang, P. Guess, and V.P. Thompson, Performance of dental ceramics challenges for improvements, J Dent Res, 90 (2011) 937-952.

[6] B.E. Pjetursson, I. Sailer, M. Zwahlen, C.H. Hammerle, A systematic review of the survival and complication rates of all-ceramic and metal–ceramic reconstructions after an observation period of at least 3 years. Part I: Single crowns, Clin Oral Implants Res., 18 (2007) 86-96.

[7] H. Wang, G. Isgro, P. Pallav, A.J. Feilzer, Fracture toughness determination of two dental porcelain with the indentation strength in bending method, Dent Mater, 23(2007) 755-759.

[8] M. Taira, Y. Nomura, K. Wakasa, M. Yamaki, A. Matsui, Studies on fracture toughness of dental ceramics, J Oral Rehabil, 17(1990) 551-563

[9] S. Al-Shehri, Relative fracture toughness and hardness of dental ceramics, Saudi Dental Journal,14 (2002) 67-72.

[10] J.F. Mansfield, X-ray analysis in the ESEM a challenge or a contradiction, Mikrochimica Acta 132 (2000) 137–143.

[11] M.Yamaoka, H.Murakami, S.Miyazaki, Diffusion and incorporation of Zr into thermally grown SiO2 on Si(1 0 0), Appl Surf Sci, 216 (2003) 223-227.

[12] J.C. Durand, B. Jacquot, H. Salehi, M. Fages, J. Margerit, F.J. Cuisinier, Confocal Raman microscopic analysis of the zirconia/feldspathic ceramic interface, Dent Mater, 28 (2012) 661-671.

[13] H.J. Kim, H.P. Lim, Y.J. Park, M.S. Vang, Effect of zirconia surface treatments on the shear bond strength of veneering ceramic, J Prosthet Dent. 105 (2011) 315-322.

[14] P.G. Coelho, J.M. Granjeiro, G.E. Romanos, M. Suzuki, N.R. Silva, G. Cardaropoli, V.P. Thompson, J.E. Lemons, Basic research methods and current trends of dental implant surfaces, J Biomed Mater Res B Appl Biomater, 88 (2009) 579-596.

[15] J.B. Quinn, G.D. Quinn, J.R. Kelly, S.S. Scherrer, Fractographic analyses of three ceramic whole crown restoration failures, Dent Mater, 21 (2005) 920-929.

[16] S.S. Scherrer, J.B. Quinn, G.D. Quinn, H.W. Wiskott, Fractographic ceramic failure analysis using the replica technique, Dental Mater, 23 (2007) 1397-1404.

[17] B. Taskonak, J. Yan, J.J.Jr Mecholsky, A. Sertgozc, A. Kocak, Fractographic analyses of zirconia-based fixed partial dentures, Dental Mater, 24 (2008)1077-1082.

[18] M.J. Tholey, M.V. Swain, N. Thiel, SEM observations of porcelain Y-TZP interface, Dent Mater, 25 (2009) 857-862.

[19] M.V. Swain, Unstable cracking (chipping) of veneering porcelain on all-ceramic dental crowns and fixed partial dentures, Acta Biomater. 5 (2009) 1668-1677.

[20] J.J. Kruzic, D.K. Kim, K.J. Koester, R.O. Ritchie, Indentation techniques for evaluating the fracture toughness of biomaterials and hard tissues. J Mech Behav Biomed, 2(2009) 384-395.

[21] J.J. Kruzic, R.O. Ritchie, Determining the toughness of ceramics from Vickers indentations

using the crack-opening displacements: an experimental study. J Am Ceram Soc., 86(2003) 1433-1436.